Journal of Cellular Automata, Vol. 3, pp. 57–79
Reprints available directly from the publisher
Photocopying permitted by license only

Packard Snowflakes on the von Neumann Neighborhood

CHARLES D. BRUMMITT[1,*], HANNAH DELVENTHAL[2]
AND MICHAEL RETZLAFF[3]

[1]*5000 N. Woodruff Ave, Milwaukee, WI 53217*
[2]*2804 N Calvert St. Apt. 1R, Baltimore, MD 21218*
E-mail: hannanole@gmail.com
[3]*319 S. Fremont Ave., Baltimore, MD 21230*
E-mail: maretzlaff@wisc.edu

Received: July 16, 2007. Accepted: July 23, 2007.

In 1984, Packard [1] introduced simple planar cellular automata to emulate the growth of snow crystals. These *Packard Snowflakes* have since been popularized by S. Wolfram and others, most recently in [2]. The present paper provides a rigorous analysis of the simplest examples: those with nearest neighbor interaction on the two-dimensional integers. In each case we determine the asymptotic density with which the spreading crystal fills the plane. For the basic *Exactly 1* rule started from a singleton, we establish alternate representations of the final state as a uniform tag system and as a substitution system.

Keywords: cellular automata, crystal growth, asymptotic density, solidification, uniform tag system, substitution system.

1 PRELIMINARIES

Introduction

Snow crystals have inspired mathematical modeling for more than a century, dating back at least as far as the early fractal known as the Koch Snowflake [3]. The details of real snowflake growth, whereby water vapor gradually freezes to form the growing crystal, are still poorly understood. An extremely simple prototype for planar growth was proposed by Packard [1]. In his cellular automaton (CA) model, each *cell* (or site) of a planar lattice changes from empty to

*E-mail: cbrummitt@wisc.edu

occupied as that location turns to ice and remains occupied thereafter. A cell "freezes" when it has one frozen neighbor, or when the number of frozen neighbors equals some prescribed higher count. Cells of the original 1984 model had six nearest neighbors, reflecting the hexagonal molecular structure of ice and observed symmetry of actual snow crystals. Subsequenct studies [2,4] include simulations on the two-dimensional intergers $\mathbb{Z}^2$ with 4 and 8 nearest neighbors, the so-called *von Neumann* and *Moore* neighborhoods, respectively.

As they grow, hexagonal Packard Snowflakes develop intricate patterns reminscient of real snowflakes (cf. Fig. 8 of [5]). Indeed, Wolfram and others have argued (e.g., in [6,7], and [2]) that the similarity demonstrates the ability of simple local interactions to capture essential features of complex natural processes. Recent advances in our understanding of real snow crystal growth, however, make it clear that the Packard rules evolve in a very different manner than do the sectored plates they ressemble at certain stages of development. More realistic lattice algorithms, based on physical principles, are currently being developed by Gravner and Griffeath [5, 8]; see those articles for an extensive bibliography of the modeling literature.

Despite their limited realism, the Packard rules are basic cellular automata with fascinating properties. Wolfram has described the patterns they generate as "intricate, if very regular" [2, p. 171]. Gravner and Griffeath [9] first provided a precise analysis of a Packard Snowflake on the Moore neighborhood and proved that it fills the plane with asymptotic density $\frac{4}{9}$. Their more recent paper [10] gives quite a complete rigorous treatment of all the original, hexagonal Packard rules.

Our objective here is to present a corresponding mathematical description for all Packard automata with the most elementary neighborhood structure: the von Neumann case. We will focus on the evolution of crystals started from a singleton, derivation of exact formulas for their cell counts at dyadic times, and calculation of asymptotic densities with which they fill the plane. Figure 1 shows a still frame of the *Exactly 1* Packard Snowflake that will be the featured example of our study. A more general analysis of asymptotic density from arbitrary finite initial seeds can be carried out using the methods of [10]. Techniques from that paper also apply to the description of macroscopic dynamics.

While mathematically rigorous, our results have been obtained after extensive experimentation. This project would not have been possible without the aid of an interactive CA simulator for visualization and data analysis. We are grateful to Mirek Wojtowicz for creating the *MCell* software [11] used throughout our research and for all the figures included here. Likewise, the reader should consider *MCell* (or some such simulator) indispensible for careful study of our work.

The paper is organized as follows. In the remainder of this Introduction, we formalize the cellular automata we will study, describe a simple transformation T that plays a key role in our analysis, and then review the familiar *Sierpinski lattice* embedded within the evolution of Packard Snowflakes.

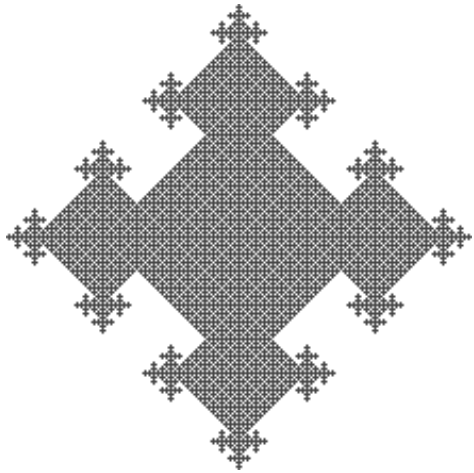

FIGURE 1
Exactly 1 at time 109 is reminiscent of a Koch Snowflake.

Section 2 quickly dispenses with the four uninteresting crystals that grow as solid diamonds. Next, Section 3 presents a recursive description of the Exactly 1 case, and shows that this crystal fills the plane with density $\frac{2}{3}$. Exactly 1 from a singleton produces an especially simple aperiodic pattern which we represent as uniform tag and substitution systems in Section 4. (These two results were mentioned without proof in [10].) Our final three sections analyze the 13, 14, and 134 crystals, respectively. In addition, Section 5 includes discussion of the closely-related cellular automaton indexed as *Rule 174* in [4].

Notation

Let us now turn to the construction and notational framework for the cellular automata we will study. Our *Packard Snowflakes* evolve on the two-dimensional integer lattice, so the crystal of frozen sites belongs to the state space

$$\mathcal{A} = \{\text{finite subsets } A \subset \mathbb{Z}^2\}.$$

Elements of A will generally be denoted by u or v and represented coordinate-wise by (x, y). The state of the crystal at time t is denoted

$$A_t = \{\text{occupied sites at time } t\}.$$

To specify whether or not a site is occupied, we write $A_t(u) = 1$ if $u \in A_t$, $= 0$ otherwise. Our analysis will focus on crystals started from a singleton; i.e., we usually set $A_0 = \{0\}$. A focus of our analysis will be the *final state*

$$A_\infty = \lim_{t \to \infty} A_t.$$

Sitewise convergence here is automatic since Packard Snowflakes *solidify*, meaning that once a cell freezes it belongs to the crystal forever.

To prescribe the dynamics of A_t, let us begin with the neighborhood of interaction. We denote the familiar nearest neighbor norms as

$$\|(x, y)\|_1 = |x| + |y|,$$

and

$$\|(x, y)\|_\infty = \max\{|x|, |y|\}.$$

This paper studies Packard Snowflakes with the *von Neumann neighborhood* of a cell u given by

$$\partial^1 u = \{v : \|v - u\|_1 = 1\}$$

It will also be convenient to introduce the *Moore neighborhood* of u

$$\partial^\infty u = \{v : ||v - u||_\infty = 1\},$$

although systematic analysis of Packard Snowflakes on this latter neighborhood is deferred to a future project. When the norm and neighborhood are clear from context, we write them simply as $||u||$ and ∂u. We also define the neighborhood of a set of cells $A \in \mathcal{A}$,

$$\partial A = \{u \in A^c : u \in \partial v \text{ for some } v \in A\}.$$

Packard Snowflakes specify whether a site joins the crystal based on how many occupied neighbors the site "sees." Thus we introduce the set of sites in ∂A that see k neighbors in A as

$$S_k = S_k(A) = \{u \in \partial A : \#(\partial u \cap A) = k\}, \quad k = 1, \ldots, 4. \tag{1}$$

The solidification rules we study are transformations $\tau_I : \mathcal{A} \to \mathcal{A}$ given by

$$\tau_I(A) = A \cup \bigcup_{i \in I} S_i,$$

where the rule index $I \subset \{1, 2, 3, 4\}$ and $1 \in I$. In words, a site u joins the crystal A if the number of occupied sites u sees belongs to I. For convenience, we abbreviate $\tau_{\{1,3\}} = \tau_{13}$, etc. The basic case τ_1 is often called the *Exactly 1* rule. We also abbreviate $\tau_I^t(A_0) = A_t^I$ for $t \leq \infty$.

It will be useful to distinguish regions of $\mathbb{Z}^2$, specifically the diamond

$$D_t = \{x : \|x\|_1 \leq t\},$$

and the box

$$B_t = \{x : \|x\|_\infty \leq t\}.$$

Started from $A_0 = \{0\}$, the crystals A_t^I exhibit a diamond-shaped outline at the end of each dyadic time interval (cf. Fig. 2). Thus it is particularly

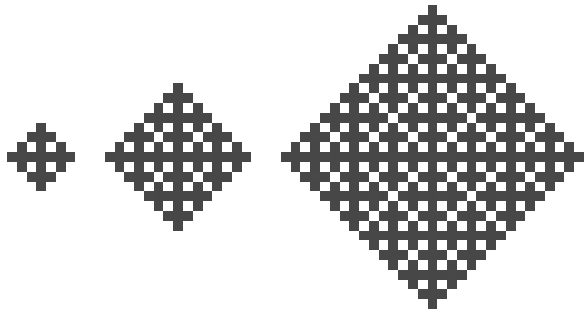

FIGURE 2
Exactly 1 from a singleton at times 3, 7, and 15.

convenient to analyze the evolution along the subsequence of times $N = N_n = 2^n - 1$, comparing the population and pattern of frozen cells to those of the full diamond D_N.

Appealing to symmetry, we will inspect the portion of crystals in the first quadrant. Hence we write, for $A \in \mathcal{A}$,

$$Q(A) = \{u = (x, y) : u \in A, x \geq 0, y \geq 0\}.$$

For brevity, set $Q_t = Q(A_t)$.

A principal goal of this paper is to compute the *asymptotic density* ρ for each τ_I. To this end, let us denote the population counts at dyadic times as

$$a_n = \#A_N, \quad q_n = \#Q_N,$$

and define

$$\rho_I = \lim_{N \to \infty} \frac{a_n}{\#D_N},$$

where I specifies the rule index of τ_I. We will see that the limit exists in every case. Methods from [10] can be applied in our setting to show that ρ satisfies the general definition of asymptotic density given in that paper and is independent of the initial finite seed A_0.

The rotation *T*

Packard Snowflakes on the von Neumann neighborhood display diamond-shaped features, reflecting the geometry of ∂^1. Rotated by 45° the crystal boundaries align horizontally and vertically, making their patterns easier to detect(see, e.g., Fig. 3). Originally motivated by computer visualization, we will see in Section 3 that this rotation T reveals especially beautiful structure of the Exactly 1 rule.

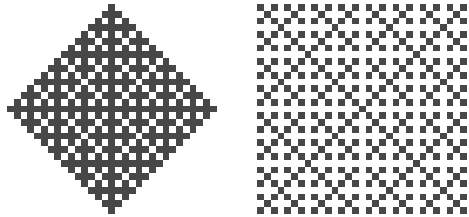

FIGURE 3
The Exactly 1 crystal (*left*) and rotated by T (*right*).

Formally, let us introduce

$$T = \begin{pmatrix} 1 & 1 \\ -1 & 1 \end{pmatrix},$$

which maps $\mathbb{Z}^2$ to the *even checkerboard* $C_e = \{(x, y) : x + y \text{ is even}\}$. In particular, note that $TD_N = B_N \cap C_e$.

Write $\tau_I^* = T\tau_I T^{-1}$ for the rotated versions of the τ_I. Note that each τ_I^* is an update rule on subsets of C_e with neighborhoods $\partial^* u = \partial^\infty u \setminus \partial^1 u$. Also, put $A_t^* = \tau^{*n} A_t$, and so on. In this manner, the rotated rules τ_I^* and their occupied sets A_t^* can be viewed as new cellular automata. Since T is one-to-one, $\#(A_N^*) = a_n$, so applying T does not affect population counts. We abbreviate the portion of the rotated crystal in the first quadrant as $Q_N^* = Q(A_N^*)$.

Iterates of the *odd checkerboard* $C_o = \{(x, y) : x + y \text{ is odd}\}$ under T will play a central role in our analysis of Exactly 1, so we will make repeated use of the following elementary facts.

Proposition 1. *Let* $(x, y) \in \mathbb{Z}^2$. *Then*

$$TC_o = D := \{(x, y) : x \text{ odd}, y \text{ odd}\}, \tag{2}$$

$$TD = 2C_o. \tag{3}$$

Proof. To check (2), let $(x, y) \in C_o$ with $x + y = 2n + 1$ for some integer n. Then

$$T\begin{pmatrix} x \\ y \end{pmatrix} = \begin{pmatrix} 2n + 1 \\ -2x + (2n + 1) \end{pmatrix},$$

the coordinates of which are both odd. Moreover,

$$T\begin{pmatrix} m - n \\ m + n + 1 \end{pmatrix} = \begin{pmatrix} 2m + 1 \\ 2n + 1 \end{pmatrix},$$

so any site with both coordinates odd is obtained from a suitable choice of x and y.

To check (3), let $(x, y) \in D$ with $x = 2m + 1$ and $y = 2n + 1$. Then

$$T \begin{pmatrix} x \\ y \end{pmatrix} = 2 \begin{pmatrix} m + n + 1 \\ n - m \end{pmatrix} \in 2C_o.$$

Conversely,

$$T \begin{pmatrix} 2a - 2k - 1 \\ 2k + 1 \end{pmatrix} = \begin{pmatrix} 2a \\ 2(2k + 1 - a) \end{pmatrix}$$

exhibits any site in $2C$ as the image of a site in D. □

In combination, (2) and (3) imply that $T^2 C_o = 2C_o$, $T^3 C_o = 2D$, $T^4 C_o = 4C_o$, ... Thus for all $k \geq 0$,

$$T^{2k} C_o = 2^k C_o \tag{4}$$

$$T^{2k+1} C_o = 2^k D. \tag{5}$$

Sierpinski embedding

The familiar *Sierpinski lattice* (or *sieve*, or *triangle*) [12] is embedded in A_∞ for all the rules τ_I we are considering (cf. Fig. 4). This structure is generated as the space-time trace of the one-dimensional XOR CA with two nearest neighbors and starting from a singleton. Vacant sites at the boundary of the "light cone" in our Packard Snowflakes (e.g., cells within the first quadrant along the line $x + y = t$ at time t) see exactly two neighbors that could be occupied. If exactly one of those neighbors is occupied, then the site solidifies since $1 \in I$ for all of our rules. In particular, the crystal advances along the

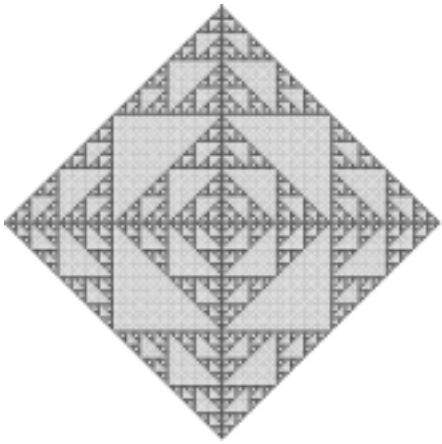

FIGURE 4
Exactly 1 with embedded Sierpinski lattices in a darker shade.

axes every update. If $2 \in I$, then τ_I fills the plane, as we will show below. If $k \in I$ with $k \geq 3$, a site on the edge of the light cone cannot solidify by the k rule since at most two neighbors can be occupied. Hence, in all cases with $2 \notin I$, the cells of each quadrant that solidify at light speed form a copy of the Sierpinski lattice.

In subsequent sections we will make use of the following well-known properties of the Sierpinski lattice in its XOR representation with neighbor set $\{-1, 1\}$:

- At time N all odd sites in $[-N, N]$ are occupied.
- At time $N + 1$ all sites are empty except $\pm(N + 1)$.
- Sites on the edge of the light cone solidify; i.e., $\pm t$ are occupied at time t.

2 THE RULES τ_I, $2 \in I$

We begin our study of von Neumann neighborhood Packard Snowflakes with the four trivial cases such that $2 \in I$; namely, $\tau_{12}, \tau_{123}, \tau_{124}, and \tau_{1234}$. Starting from a singleton these rules cover D_t at time t.

Proposition 2. *Suppose* $2 \in I$ *and* $A_0 = \{0\}$. *Then* $A^I_\infty = \mathbb{Z}^2$ *and* $\rho_I = 1$.

Proof. We show that for any $t \geq 0$,

$$A_t = D_t. \tag{6}$$

At time $t = 1$ the cells of $A_1 = \{(0, 0), (0, 1), (1, 0), (0, -1), (-1, 0)\} = D_1$ are frozen. Assuming (6), at time $t + 1$ any cell (x, y) of $Q(\partial D_t)$ satisfies $x + y = t + 1$. If $x = 0$ or $y = 0$, then (x, y) has one occupied neighbor in A_t at $(x - 1, 0)$ or $(y - 1, 0)$, respectively. If $x, y \neq 0$, then (x, y) has 2 occupied neighbors at $(x, y-1)$ and $(x-1, y)$. In either case (x, y) solidifies. (Note that since all cells within the light cone D_t solidify due to the 1 or 2 condition, the 3 and 4 conditions are superfulous.) Thus $Q(D_{t+1}) = Q(A_{t+1})$ By symmetry, (6) holds for all t. In particular, $A_\infty = \mathbb{Z}^2$ and $\rho_I = 1$. □

3 THE EXACTLY 1 RULE

We now derive an exact population formula for the simplest non-trivial nearest-neighbor Packard Snowflake started from a singleton, showing that it fills the plane with density $\frac{2}{3}$.

Proposition 3. *For* τ_1, *if* $A_0 = \{0\}$ *the number of occupied cells at time* $N = 2^n - 1$ *is* $a_n = \frac{4^{n+1}-1}{3}$. *Hence* $\rho_1 = \frac{2}{3}$.

Let us begin by proving the population formula for the rotated Exactly 1 rule τ_1^*, since this is easier to visualize, and then transform back to τ_1. Recall that a_n denotes the population of the entire crystal at time $N = 2^n - 1$. Let $Q_n = Q(A^*_{N_n})$ be the portion of the rotated crystal in the first quadrant, $q_n = \#Q_n$ its population. By direct enumeration, $a_1 = 5$, $a_2 = 21$, $a_3 = 85, \ldots$; $q_1 = 2$, $q_2 = 6$, $q_3 = 22, \ldots$. In fact, $\#Q(A_t^* \cap D_N)$ does not change after time $t = N_n$; i.e., the final configuration on D_N is attained at time N, but we defer the verification of this until the proposition is proved.

First, we claim that Q_{n+1} consists of four rigid transformations of Q_n (see Fig. 5). Assuming the claim for the moment, the three new clones of Q_n branch from the seed at $(2^n, 2^n)$ in the NW, NE and SE directions. Since q_{n+1} counts this seed only once,

$$q_{n+1} = 4q_n - 2. \tag{7}$$

The whole crystal A_n consists of 4 copies of Q_n, but the origin is counted three too many times in a_n. Hence

$$a_n = 4q_n - 3. \tag{8}$$

Using the initial data to solve (7) and (8), we have

$$q_n = \frac{4^n + 2}{3}, \quad a_n = \frac{4^{n+1} - 1}{3}, \tag{9}$$

as desired. Since the box $B_n = [-N, N]^2$ has order 4^{n+1} sites, it follows that the asymptotic density ρ_1^* of the rotated crystal equals $\frac{1}{3}$. Applying T^{-1} to recover the original orientation conserves the crystal cell count but halves the

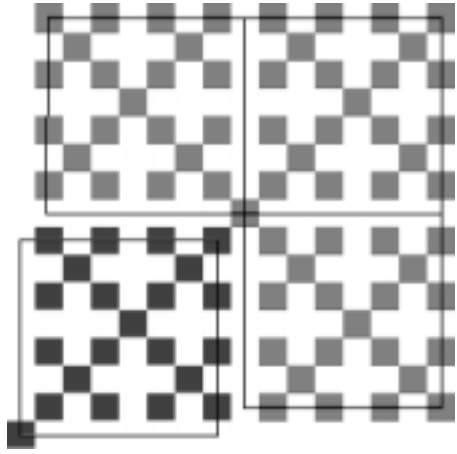

FIGURE 5
The first quadrant of the rotated Exactly 1 crystal at time 15. The lighter cells, i.e., the new growth from time N_3 to N_4, are rigid transformations of the darker cells grown by time N_3.

area. (T dilates the original pattern by a factor of 2 by inserting a permantently empty cell between each pair of cells.) Hence $\rho_1 = \frac{2}{3}$.

Next we prove the claimed cloning structure of Q_{n+1} in terms of Q_n by induction. Since A_t^* is symmetric started from a singleton, the same analysis applies to the other three quadrants. Let us begin with the boundaries of Q_n.

Lemma 1. *A_∞^* contains no cells on the x- or y-axes except the origin.*

Proof. Because the dynamics within the four quadrants of the plane are symmetric, sites on the axes have either 0, 2, or 4 occupied neighbors at all times, so they never join the crystal. □

Lemma 2. *A_∞^* contains no cells in the rows and columns $\{N+1\} \times [1, N]$ and $[1, N] \times \{N+1\}$.*

Proof. Since halves of two Sierpinski lattices are embedded in $Q(A_\infty^*)$, cells of $\{N\} \times [1, N]$ and $[1, N] \times \{N\}$ are alternately occupied and empty. Cells in the next row and column (i.e., in $[1, N] \times \{N+1\}$ and in $\{N+1\} \times [1, N]$, respectively) look to their corner neighbors and see either 0 or 2 occupied cells. According to τ_1^*, these cells never join the crystal. □

Lemmas 1 and 2 determine the boundaries for the evolution of Q_n, while the following property gives rise to recursive structure. See Fig. 6.

Lemma 3. *Under τ_1^*, a ray of occupied cells travels from $(0, 0)$ at speed 1 in the NE direction. That is, (t, t) joins the rotated crystal at time t.*

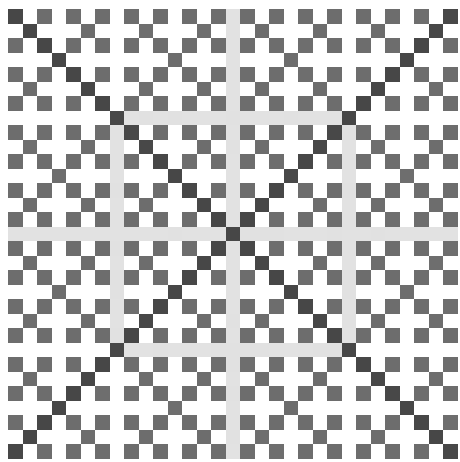

FIGURE 6
Depiction of the three lemmas used to analyze growth of τ_1^*. The empty cells guaranteed by Lemmas 1 and 2 are light gray, while the darkest cells are occupied by Lemma 3. Together these determine the boundaries of dyadic regions.

Proof. Observe that $(1, 1)$ joins the crystal at times 1. Assume (t, t) joins at time t. At this time, the light cone, i.e., the set of sites that can be affected by the initial seed, is $C_t := B_t \cap C_e$. Site $(t+1, t+1)$, which is outside the light cone, has only one neighbor that could be occupied: namely, (t, t). Hence, if (t, t) is occupied at time t, then $(t+1, t+1)$ joins at time $t+1$ according to τ_1^*. The lemma follows by induction. □

Returning to the proof of the claimed cloning process, we iterate τ_1^* to time N_n. By Lemma 3, there is a new "seed," or occupied cell, at (N_n+1, N_n+1). By Lemma 1, there is a boundary of empty cells to the left and below this seed (namely, in $\{N_n+1\} \times [1, N_n]$ and in $[1, N_n] \times \{N_n+1\}$). Therefore, evolution from this seed is analogous to that from the origin. More precisely, because there are exactly the same boundary conditions as at time 0 (the row and column of empty cells on the axes as established by Lemma 1), the crystal will grow exactly as before within the boundaries. Because the boundary conditions NE, NW, and SE of the seed are identical to those at the origin, the configuration Q_n will be exactly copied NE, NW, and SE of the new seed. The new squares are:

$$\begin{aligned} [N_n+1, N_n+1] \times [N_{n+1}, N_{n+1}] &\quad \text{for the NE copy,} \\ [1, N_n+1] \times [N_n+1, N_{n+1}] &\quad \text{for the NW copy,} \\ [N_n+1, 1] \times [N_{n+1}, N_n+1] &\quad \text{for the SE copy.} \end{aligned}$$

Thus, the rotated Exactly 1 rule evolves recursively as described above.

Finally, we return to the claim that under τ_1^*, the final configuration on B_N is attained at time N (i.e., $A_N^* = A_\infty^* \cap B_N$). By symmetry, it suffices to consider the first quadrant; empty cells guaranteed by Lemma 1 preclude interaction across the axes.

Iterate τ_1^* to time $N_2 = 3$. At the next iteration, a new seed forms at $(4, 4)$. By Lemma 1, sites in the row and column to the left and below this seed (i.e., in $[0, 3] \times \{4\}$ and in $\{4\} \times [0, 3]$) never join A_∞. Because the boundaries of $Q(B_3)$ never join A_∞, sites in $Q(B_3)$ are not affected by sites outside $Q(B_3)$ after time 3. Evidently, sites in $Q(B_3)$ are not affected by sites *inside* $Q(B_3)$ after time 3 since one can observe that the configuration on $Q(B_3)$ at time $N_2 = 3$ equals the configuration on $Q(B_3)$ at time $N_3 = 7$. This shows that the final configuration on B_3 is attained at time $N = 3$.

Next, assume the claim holds on B_{N_n} at time N_n. Again appealing to symmetry, we consider only the first quadrant. According to the recursion of τ_1^* proved above, the configuration on $Q(B_{N_{n+1}})$ consists of $Q(B_{N_n})$ and three rigid transformations of $Q(B_{N_n})$. The original $Q(B_{N_n})$ satisfies the claim by the induction hypothesis. Each of the three new copies of $Q(B_{N_n})$ begins from the seed $(2^n, 2^n)$ at time $N_n + 1$ and grows exactly as Q_n did from the origin because they have the same boundaries. Hence the three copies attain their

final configuration at time N_{n+1} in the same way that Q_n did at time N_n, which completes the proof.

Since the rotation T is an isomorphism of dynamics on the ∂^1 and ∂^* neighborhoods, the analogous result (9) for the Exactly 1 rule τ_1 is immediate.

4 OTHER CHARACTERIZATIONS OF A^*_∞ AND A_∞ FOR τ_1

Started from a singleton, the final states of all Packard Snowflakes on the von Neumann neighborhood are *exactly solvable* in the sense of [10]. Exactly 1, structurally the simplest (non-trivial) case, admits three alternate representations to the recursion of the last section.

The binary rule

First, there is a simple description of sites (x, y) belonging to the final state in terms of the binary representations of x and y.

Proposition 4. *A^*_∞ satisfies the binary rule:*

$$(x, y) \textit{ is occupied iff } \begin{cases} x = y = 0, \textit{ or } x, y \neq 0 \textit{ and the greatest} \\ \textit{powers of 2 dividing } x \textit{ and } y \textit{ are the same.} \end{cases} \tag{10}$$

Proof. By symmetry, it suffices to check (10) in the first quadrant. Lemma 1 establishes the binary rule on $\{x = 0 \text{ or } y = 0\}$. It can also easily be checked that the occupied set of the binary rule on $Q(B_3)$ agrees with Q_3. Now we assume the binary rule agrees with Q_n on $Q(B_n)$ and show that it also agrees with Q_{n+1} on $Q(B_{n+1})$. The square $[0, 0] \times [N_n, N_n]$ is cloned into three squares NE, NW, and SE of the new seed by translating and rotating by $0°$, $+90°$, and $-90°$, respectively, as described in Section 3. Since τ_1^* is symmetric across the $x = 0$, $y = 0$ and $y = \pm x$ axes, the configuration in the NW square is Q_n reflected across the line $x = N_n$. Likewise, the SE square is Q_n reflected across the line $y = N_n$. Thus we can choose the cloning to map (x, y) in $[0, 0] \times [N_n, N_n]$ to $(x, y) + (\epsilon_1 2^n, \epsilon_2 2^n)$, where $\epsilon_1 = \epsilon_2 = 1$ for the NE square, $\epsilon_1 = 0, \epsilon_2 = 1$ for the NW square, and $\epsilon_1 = 1, \epsilon_2 = 0$ for the SE square.

Take any $(x, y) \in [1, 1] \times [N_n, N_n]$. Clearly, the greatest dyadic divisors of both x and y are between 1 and 2^{n-1}. Thus, adding 2^n to x or y merely puts a 1 on the left end of its binary representation. If the greatest powers of two that divide x and y are the same (different), then after adding 2^n to either or both of x and y, their greatest power of two divisors are still the same (different). Hence the binary rule holds on the set $[1, 1] \times [N_{n+1}, N_{n+1}] \setminus \{x = 2^n \text{ or } y = 2^n\}$.

In the remaining cases, the greatest dyadic divisor of one of x and y is 2^n and the other is at most 2^n. If they both are 2^n, which corresponds to the site $(2^n, 2^n)$, then x and y share the same greatest dyadic divisor, so the site is

occupied. (This is the "seed" mentioned in the cloning proccess earlier.) If, on the other hand, the greatest dyadic divisor of one of x and y is less than 2^n, then they have different greatest dyadic divisors, so the cell is empty. (This corresponds to the boundaries of empty cells established in Lemmas 1 and 2.) Hence the binary rule holds on all of $[0, 0] \times [N_{n+1}, N_{n+1}]$. By induction the rotated Exactly 1 crystal A_n^* satisfies the binary rule. □

A_∞^* in terms of dilated odd checkerboards

Next, it turns out that the union of all odd iterates of the odd checkerboard C_o under T yields the rotated Exactly 1 pattern.

Proposition 5. $A_\infty^* = \bigcup_{k=0}^\infty T^{2k+1} C_o = \bigcup_{k=0}^\infty 2^k D$.

Proof. Recall the definition of D from Proposition 1 and observe that

$$2^k C_o = \{(x, y) : (2^k | x, 2^{k+1} \nmid x, 2^{k+1} | y) \text{ OR } (2^k | y, 2^{k+1} \nmid y, 2^{k+1} | x)\}, \tag{11}$$

$$2^k D = \{(x, y) : 2^k | x, 2^k | y, 2^{k+1} \nmid x, 2^{k+1} \nmid y\}. \tag{12}$$

In words, $2^k D$ is the set of (x, y) such that the greatest dyadic divisor of both x and y is 2^k. By (3) the greatest dyadic divisors of both coordinates of sites in D are 2^0, so multiplying both by 2^k makes their greatest dyadic divisors both 2^k as claimed. Similarly, $2^k C_o$ is the set of (x, y) such that the greatest dyadic divisor of one of x and y is 2^k and the greatest dyadic divisor of the other is greater than 2^k. Since sites in C_o have one coordinate odd and the other even, after multiplying both x and y by 2^k the greatest dyadic divisors are again as claimed.

Now recall (4) and (5). Take any $(x, y) \in \mathbb{Z}^2 \setminus \{\mathbf{0}\}$, and consider the possibilities in (11) and (12). If $x = 0$ and $y \neq 0$, then $(x, y) \in T^{2k} C_o = 2^k C_o$, where k is the greatest power of two dividing y. Likewise, if $x \neq 0$ and $y = 0$, then $(x, y) \in T^{2k} C_o = 2^k C_o$, where k is the greatest power of two dividing x. Otherwise $x \neq 0$, $y \neq 0$. Let 2^m and 2^n be the greatest powers of two dividing x and y, respectively. If $m = n$, then $(x, y) \in T^{2m} D = 2^m D$ only; if $m > n$, then $(x, y) \in T^{2n} C_o = 2^n C_o$ only; if $n > m$, then $(x, y) \in T^{2m} C_o = 2^m C_o$ only. Since $TC_o = D$, the $T^k C_o$ partition $\mathbb{Z}^2 \setminus \{\mathbf{0}\}$.

Let $A'_\infty = \bigcup_{k=0}^\infty T^{2k} C_o$ and $B'_\infty = \bigcup_{k=0}^\infty T^{2k+1} C_o$. Then B'_∞ agrees with the occupied set of the binary rule by (12) and A'_∞ and B'_∞ also partition $\mathbb{Z}^2 \setminus \{\mathbf{0}\}$. We know A_∞^* satisfies the binary rule (10), so $A_\infty^* = B'_\infty$ as desired. □

Corresponding results for the final state A_∞ of the original Exactly 1 rule are now immediate consequences.

Corollary 1. *The limit set of* τ_1 *is* $A_\infty = \bigcup_{k=0}^\infty T^{2k} C_o = \bigcup_{k=0}^\infty 2^k C_o$.

Proof. Apply T^{-1} to Proposition 5. □

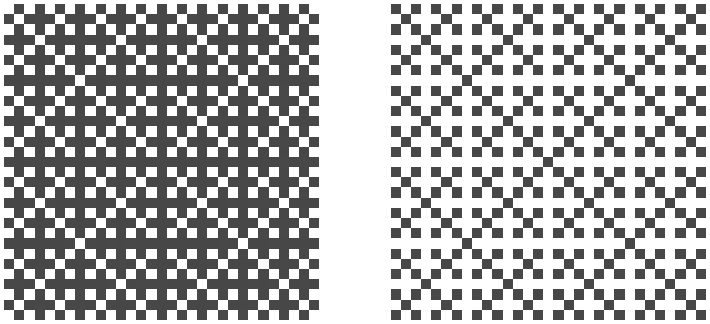

FIGURE 7
A_∞ (*left*) and TA_∞ (*right*) are complementary off $\mathbf{0}$.

Corollary 2. *A_∞ satisfies the complementary binary rule:*

$$(x, y) \text{ is occupied iff } \begin{cases} x = 0 \text{ or } y = 0, \text{ or } x, y \neq 0 \text{ and the} \\ \text{greatest powers of 2 dividing } x \text{ and } y \text{ differ.} \end{cases} \tag{13}$$

Proof. Abbreviate $A^\dagger$ for the occupied set of the complementary binary rule. We showed above that if $u \in T^{2k}C_o$ for some k then $u \in A^\dagger$, and if $u \in T^{2k}D$ for some k then $u \notin A^\dagger$. Since the $T^{2k}C_o$ and $T^{2k}D$ partition $\mathbb{Z}^2 \setminus \mathbf{0}$, $\bigcup_{k=0}^{\infty} T^{2k}C_o = A^\dagger$. By Corollary 1, $A_\infty = A^\dagger$. □

Combining the structural properties now established, we arrive at a remarkable inversion property for A_∞ under 45° rotation, as illustrated in Fig. 7.

Corollary 3. *The limit sets A_∞ and A_∞^* of τ_1 and τ_1^*, respectively, are complementary away from the origin.*

Proof. This is immediate from the observation above that A'_∞ and B'_∞ partition $\mathbb{Z}^2 \setminus \mathbf{0}$. □

We remark that Corollary 1 provides an alternate proof that $\rho_1 = \frac{2}{3}$. Namely, since $A_\infty = \bigcup_{k=0}^{\infty} T^{2k}C_o$, since applying T^2 moves cells 4 times further apart, and since the checkerboard C_o has density $\frac{1}{2}$, the asymptotic density of A_∞ is $\rho_1 = \frac{1}{2} + \frac{1}{2} \cdot \frac{1}{4} + \frac{1}{2} \cdot \frac{1}{4^2} + \ldots = \frac{2}{3}$. Corollary 3 then implies that the asymptotic density ρ_1^* of the rotated crystal equals $\frac{1}{3}$.

A substitution system

In addition, the final state of Exactly 1 is generated by an extremely simple *substitution system* (or *L-system*). The scheme for τ_1 in the first quadrant is shown in Fig. 8.

By Corollary 3, reversing black and white yields the system for τ_1^*, as in Fig. 9.

FIGURE 8
Substitution system for τ_1.

FIGURE 9
Substitution system for τ_1^*.

FIGURE 10
Evolution of the substitution system for τ_1 in the first quadrant.

FIGURE 11
Evolution of the substitution system for τ_1^* in the first quadrant.

The first four iterates of the two substitution systems are shown in Figs. 10 and 11.

To show that the scheme of Fig. 8, started from a single black cell, generates $Q(A_\infty)$, we prove agreement with the complementary binary rule (13) by induction. It is easy to check that the pattern generated by two iterations of the substitution scheme equals $Q(B_3) \cap A_\infty$, as shown in the middle frame of Fig. 10. Assume next that the pattern after n iterations agrees with (13) on $Q(B_{N_n})$. Take any (x, y) in the pattern generated by n iterations of the substitution system. This scheme maps (x, y) to $(2x, 2y)$, $(2x+1, 2y)$, $(2x, 2y+1)$, and $(2x + 1, 2y + 1)$. If (x, y) is occupied, i.e., the greatest powers of two dividing x and y differ, then the greatest powers of two dividing $2x$ and $2y$ still differ, so $(2x, 2y)$ is occupied. The sites $(2x + 1, 2y)$ and $(2x, 2y + 1)$ consist of an odd and an even, so their greatest dyadic divisors differ, and hence these sites are also occupied. The site $(2x + 1, 2y + 1)$ consists of two odds, which share the same greatest dyadic divisor of 1, so this site is empty. Alternatively, if (x, y) is empty, i.e., the greatest powers of two dividing x and y are the same, then the greatest powers of two dividing $2x$ and $2y$ are still the same,

so $(2x, 2y)$ is empty. The sites $(2x+1, 2y)$ and $(2x, 2y+1)$ consist of an odd and an even, so their greatest dyadic divisors differ, and hence these sites are occupied. Finally, the site $(2x+1, 2y+1)$ consists of two odds, which share the same greatest dyadic divisor of 1, so this site is empty. Agreement for all n follows.

5 THE τ_{14} RULE

Let us turn to the Packard Snowflake generated by τ_{14}. We will view this CA as a perturbation of Exactly 1, using results from the last two sections to show that $A_\infty^{14} = \mathbb{Z}^2$. Snapshots in [2, p. 171] strongly suggest as much, although not even a conjecture is stated explicitly there.

We start by noting that the only effect of the 4 condition in τ_{14} is to fill vacant sites once they are completely surrounded by occupied neighbors. Thus, the 4 condition does not interfere with the evolution under τ_1. Properly formulated, this observation is valid for any of the Packard rules: for $\Lambda \subset \{1, 2, 3\}$, first running τ_Λ for $t-1$ steps and then "filling the holes" with $\tau_{\Lambda 4}$ is the same as running $\tau_{\Lambda 4}$ for t steps. The proof we offer is topological.

Proposition 6. *For $t \geq 1$ and $\Lambda \subset \{1, 2, 3\}$, $\tau_{\Lambda 4}^t = \tau_{\Lambda 4} \tau_\Lambda^{t-1}$.*

To prove the proposition we will make use of the following identities:

Lemma 4. *For $\Lambda \subset \{1, 2, 3\}$,*

$$\tau_{\Lambda 4} = \tau_\Lambda \tau_4$$
$$\tau_4 \tau_{\Lambda 4} = \tau_4 \tau_\Lambda .$$

Assuming the lemma for now, the proposition follows by an easy induction:

$$\tau_{\Lambda 4}^{t+1} = \tau_{\Lambda 4} \tau_{\Lambda 4}^t = \tau_{\Lambda 4}^2 \tau_\Lambda^{t-1} = \tau_\Lambda \tau_4 \tau_{\Lambda 4} \tau_\Lambda^{t-1} = \tau_\Lambda \tau_4 \tau_\Lambda \tau_\Lambda^{t-1} = \tau_{\Lambda 4} \tau_\Lambda^t . \quad \square$$

Write $S_\Lambda = \cup_{i \in \Lambda} S_i$. According to (1), to prove Lemma 4 we must show equivalently that

$$S_\Lambda(A) = S_\Lambda(A \cup S_4(A)), \tag{14}$$
$$S_4(A) \cup S_4(A \cup S_\Lambda(A) \cup S_4(A)) = S_4(A \cup S_\Lambda(A)). \tag{15}$$

To this end, we derive a more basic identity.

Lemma 5. *For $A_0, A_1 \in \mathcal{A}$ such that $A_0^c \cap \partial A_1 = \varnothing$,*

$$S_\Lambda(A_0 \cup A_1) = S_\Lambda(A_0) \cap A_1^c .$$

Proof. $\partial(A_0 \cup A_1) = (\partial A_0 \cap A_1^c) \cup (\partial A_1 \cap A_0^c)$. By hypothesis, and elementary properties of S_Λ,

$$\begin{aligned} S_\Lambda(A_0 \cup A_1) &= \{x \in \partial A_0 \cap A_1^c : \#\{\partial x \cup (A_0 \cap A_1)\} \in \Lambda\} \\ &= \{x \in \partial A_0 \cap A_1^c : \#\{y \in (A_0 \cap A_1) : x \in \partial y\} \in \Lambda\} \\ &= \{x \in \partial A_0 \cap A_1^c : \#\{y \in A_0 : x \in \partial y\} \in \Lambda\} \\ &= \{x \in \partial A_0 \cap A_1^c : \#\{\partial x \cap A_0\} \in \Lambda\} \\ &= S_\Lambda(A_0) \cap A_1^c. \end{aligned}$$

Note that the third equality holds since $x \in \partial A_0$ implies $x \in A_0^c$, whereas $y \in A_1$ and $x \in \partial y$ imply $x \in \partial A_1$, contradicting the hypothesis. □

Now to show (14), set $A_0 = A$ and $A_1 = S_4(A)$ in Lemma 5. Since $\partial S_4(A) \subset A$ the assumption of the lemma is satisfied. Thus,

$$S_\Lambda(A \cup S_4(A)) = S_\Lambda(A) \cap S_4(A)^c = S_\Lambda(A) \cap A^c = S_\Lambda(A)$$

as desired. For (15), set $A_0 = A \cup S_\Lambda(A)$ and $A_1 = S_4(A)$ in Lemma 5. Again the hypothesis holds, so

$$S_4(A \cup S_\Lambda(A) \cup S_4(A)) = S_4(A \cup S_\Lambda(A)) \cap S_4(A)^c = S_4(A \cup S_\Lambda(A)),$$

this last since $S_4(A \cup S_\Lambda(A)) \subset S_4(A)^c$. It remains to check that $S_4(A) \subset S_4(A \cup S_\Lambda(A))$. Suppose $x \in S_4(A)$. If $x \notin S_4(A \cup S_\Lambda(A))$, then $S_4(A)$ and $S_\Lambda(A))$ are not disjoint, a contradiction. □

Proposition 6 lets us analyze the solidification of A_t^{14} by determining which cells are added to A_t^1. We can extend this analysis to the correspnding final states by applying a simple continuity result.

Lemma 6. *If $A_t \to A_\infty$, then $\tau_\Lambda(A_t) \to \tau_\Lambda(A_\infty)$.*

Proof. Fix $u \in \mathbb{Z}^2$ and write $\bar{\partial} u = u \cup \partial u$. The convergence $A_t \to A_\infty$ implies that

$$A_t \cap \bar{\partial} u = A_\infty \cap \bar{\partial} u \quad \text{eventually in } t. \tag{16}$$

For t such that (16) holds,

$$(\tau_\Lambda(A_t))(u) = (\tau_\Lambda(A_\infty))(u).$$

Therefore, $\tau_\Lambda(A_t) \to \tau_\Lambda(A_\infty)$. □

In our analysis of the Exactly 1 rule we showed that cell (x, y) is not a member of A_∞^1 if and only if x and y share the same greatest power of 2

divisor. We also saw that the same condition characterizes membership in $A_N \cap D_N$. Let

$$x = \sum_{i=0}^{\infty} 2^i x_i, \quad y = \sum_{j=0}^{\infty} 2^j y_j$$

with $x_i, y_j \in \{0, 1\}$. Suppose $(x, y) \notin A^1_\infty$. Then there exists $k \geq 0$ such that $x_k = y_k = 1$ and $x_i = y_i = 0$, for $i < k$. In particular, the odd-even parities of x and y agree. Hence the four neighbors of (x, y) have coordinates with different parity. Thus $S_4(A^1_\infty) = (A^1_\infty)^c$. Combining Proposition 6 with Lemma 6,

$$A^{14}_\infty = \lim_{t\to\infty} \tau^t_{14}(A_0) = \lim_{t\to\infty} \tau_{14}(\tau^{t-1}_1(A_0)) = \tau_{14}(A^1_\infty) = \mathbb{Z}^2. \tag{17}$$

In particular, $\rho_{14} = 1$.

In similar fashion, one can show that

$$A^{14}_{N+1} = D_N \cup \{(\pm(N+1), 0), (0, \pm(N+1))\}.$$

Another variant of Exactly 1

Packard and Wolfram [4, Section 2] discussed a CA related to Exactly 1 that they incorrectly identified as a solidification rule. Namely, *Rule 174* (according to their numbering scheme) is the modification of τ_1 in which a vacant cell becomes occupied if exactly one of its four neighbors is occupied while an occupied cell becomes empty if all four neighbors are occupied. Let us denote this CA map as τ_{PW} and its final state from a singleton as A^{PW}_∞. In much the same way as for Packard Snowflakes, one can verify the analog of Proposition 6,

$$\tau^n_{PW} = \tau_{PW}\tau^{n-1}_1. \tag{18}$$

We omit the proof. Proceeding as in (17), we conclude from (18) that $A^{PW}_\infty = A^1_\infty \setminus A^\circ_\infty$, where A°_∞ consists of all sites in A^1_∞ with four neighbors in A^1_∞. Recall the decomposition of Corollary 1 and the complementary binary rule of Corollary 2. Note that $C_o \notin A^\circ_\infty$ since two neighbors of any site in the odd checkerboard have both coordinates odd. Moreover, for any $k \geq 1$, $2^k C_o \in A^\circ_\infty$ since the coordinates of all four neighbors of any site in the dilated odd checkerboard have opposite parity. We conclude that Rule 174 has asymptotic density $\frac{1}{2}$ and C_o as its final state. One can also show that

$$A^{PW}_{N+1} = (C_o \cap D_N) \cup \{(\pm(N+1), 0), (0, \pm(N+1))\}.$$

6 THE τ_{13} RULE

Intriguingly, although the patterns generated by τ_{13} differ considerably from those of τ_1 (cf. Fig. 12), the populations at dyadic times, and hence the asymptotic densities, are identical.

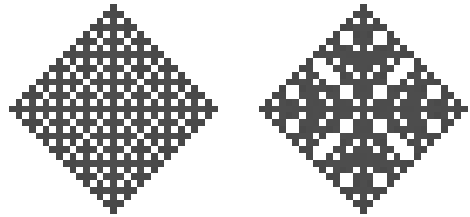

FIGURE 12
Comparison of τ_1 and τ_{13}. Cell counts are both 341 after 15 iterations from a singleton.

Proposition 7. *For τ_{13}, if $A_0 = \{0\}$ the number of occupied cells at time $N = 2^n - 1$ is $a_n = \frac{4^{n+1}-1}{3}$, and so $\rho_{13} = \frac{2}{3}$.*

As we did for Exactly 1, let us begin by deriving the population formula for the rotated rule τ_{13}^* and then transform back to τ_{13}. Again let $a_n = a_n^* = \#A_N^*$ be the population of the entire rotated crystal at time N, q_n the population of the portion of the rotated crystal in the first quadrant. Directly enumerating the first few cell counts shows that they are the same as for τ_1^*: $a_1 = 5$, $a_2 = 21$, $a_3 = 85, \ldots$; $q_1 = 2$, $q_2 = 6$, $q_3 = 22, \ldots$.

Once more, our strategy is to analyze the cloning of dyadic blocks. Whereas τ_1 reproduces square regions simply, the more intricate evolution of τ_{13} reproduces *triangular* regions. Thus we divide $Q(B_{N_{n+1}})$ into six lattice triangles and one square, as shown in Fig. 13:

$$\begin{aligned}
&\text{(I)}\ y > 0, x < N_n, y < x;\\
&\text{(II)}\ y < N_n, x > 0, y > x;\\
&\text{(III)}\ y \geq N_n + 1, x > 0, y < -x + N_{n+1} + 1;\\
&\text{(IV)}\ y < N_{n+1} + 1, x < N_n + 1, y > -x + N_{n+1} + 1;\\
&\text{(V)}\ x \geq N_n + 1, y > 0, y < -x + N_{n+1} + 1;\\
&\text{(VI)}\ x < N_{n+1} + 1, y < N_n + 1, y > -x + N_{n+1} + 1;\\
&\text{(VII)}\ [N_n + 1, N_{n+1}] \times [N_n + 1, N_{n+1}]
\end{aligned}$$

Again we abbreviate $Q_n = Q(A_{N_n}^*)$. Whereas for τ_1 we used the configuration on a square, Q_n, as the fundamental cloning object, for τ_{13} we instead use the configuration in triangular region I. We claim that Q_{n+1} consists of eight rigid transformations of the configuration in I and four rigid transformations of the diagonal $y = x$ ($0 \leq x \leq N_n$), with some overlap (cf. Fig. 13).

Denote the population in each of the seven regions as $p_I = \#(A_\infty^* \cap I)$, etc., and let $d = N + 1$ be the population of the diagonal $y = x$ ($0 \leq x \leq N_n$). By symmetry, $p_I = p_{II}$, so $q_n = 2p_I + d$.

Due to the embedded Sierpinski Lattice, the lines $[0, N] \times \{N\}$ and $\{N\} \times [0, N]$ consist of alternating occupied and empty cells. Under τ_{13}^*,

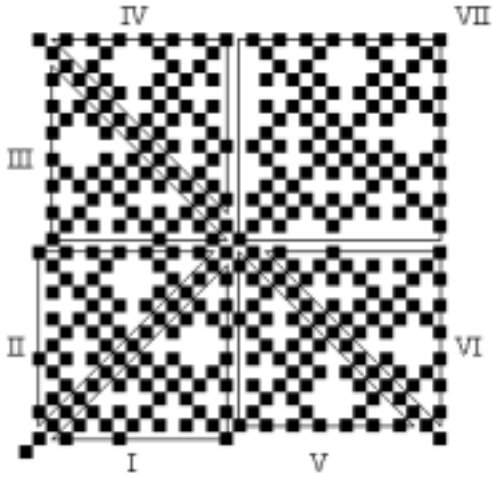

FIGURE 13
Seven regions for the analysis of τ_{13}.

these boundaries bahave equivalently to empty rows. At time $N + 1$ a seed forms at $(N + 1, N + 1)$, which belongs to region VII only. By reasoning similar to that for Lemma 1, Q_n (i.e., the configuration on the union of regions I, II, and the diagonal adjoining them) copies exactly into region VII. Since after time $N + 1$ the $N \times N$ squares NW and SE of the seed evolve for time N with boundary conditions equivalent to those at the origin at time 0, a solid diagonal advances at lightspeed in both directions along the line $y = -x + N_{n+1} + 1$. Since the seed $(N + 1, N + 1)$ belongs to VII, the population of the two diagonals separating III from IV and V from VI is $2d - 2$. Hence $q_{n+1} = 4p_I + 2d + p_{III} + p_{IV} + p_V + p_{VI} + 2d - 2$.

Since the segments $[0, N] \times \{N\}$ and $\{N\} \times [0, N]$ behave like boundaries of empty cells under the 1 or 3 rule, the boundary conditions for growth into regions III and V starting at the seed $(N + 1, N + 1)$ are identical to the conditions for growth into I and II starting from $(1, 1)$ at time 1. However, the boundary conditions for growth into IV and VI starting from $(N + 1, N + 1)$ are identical to the conditions starting from $(0, 0)$ at time 0 growing into regions I and II. Because of this, the configurations on triangles III and V are shifted by $(+1, -1)$ and $(-1, +1)$, respectively. In other words, one can imagine that the growth into region I from the seed $(0, 0)$ is identical to the growth into III from a seed at $(N_n + 2, N_n)$ rather than from $(N_n + 1, N_n + 1)$. Likewise, the growth into region I from $(0, 0)$ is identical to the growth into V from $(N_n, N_n + 2)$. These shifts do not affect the population of the rigid transformations of the configuration in region I. Hence $p_I = p_{III} = p_{IV} = p_V = p_{VI}$.

Putting all this together, we obtain

$$\begin{aligned} q_{n+1} &= 8p_I + 4d - 2 = 4(2p_I + d) - 2 \\ &= 4q_n - 2. \end{aligned}$$

This difference equation and initial data are the same as for Exactly 1, so again (8) and (9) hold in the new setting and the asymptotic densities of the rotated rule τ_{13}^* and original rule τ_{13} are $\frac{1}{3}$ and $\frac{2}{3}$, respectively.

The proof by induction of the recursive evolution for τ_{13}^* is analogous to the proof for τ_1^*, so we will skip the details. The boundary conditions described above determine the growth within triangles III through VI.

7 THE τ_{134} RULE

To conclude the paper we turn to the final Packard Snowflake on the von Neumann neighborhood, generated by τ_{134}. We view this case as a perturbation of τ_{13}, just as we considered τ_{14} a perturbation of τ_1. By Proposition 6,

$$\tau_{134}^t = \tau_{134}\tau_{13}^{t-1}.$$

Thus we can determine A_∞^{134} by filling in the holes in A_∞^{13}. Moreover, the boundary conditions for evolution of τ_{13} in regions I–VII and the cloning structure within those regions can be verified for τ_{134} in the same way. However, the population of τ_{134} has extra contributions from the 4 condition along "seams" between regions I and V, between regions II and III, and at four additional sites (cf. Fig. 14).

Let q_n be the quadrant population count of τ_{134}, p_I the count in region I, and $d = N + 1$ the diagonal population as in the previous section. Now $q_n = 2p_I + d + 2$, since additional cells are added at $(2, 0)$ and $(0, 2)$ by the 4 condition. The modified recursion is

$$q_{n+1} = 8p_I + (4d - 2) + (s_n + 4), \tag{19}$$

where $s_n + 4$ represents the contribution from sites along the above-mentioned seams and four additional sites. Simplifying, we get $q_{n+1} = 4q_n + s_n - 6$.

A final lemma now evaluates the seam correction.

Lemma 7. *There are $2^n - 1$ occupied sites forming a period 2 sequence along the boundary of Q_n that are candidates to fill in by the 4 condition, but $2n - 1$ of these are already filled in by τ_{13}. Thus $s_n = 2^n - 2n$.*

Proof. The seams $y = N_n + 1$, $0 \le x \le N_n + 1$; and $x = N_n + 1$, $0 \le y \le N_n + 1$ have a total of $2^{n+1} - 1$ cells. Due to the shifted recursion for τ_{13}, there are cells alternating between occupied and empty on both sides of the seams. However, the $2n - 1$ cells at $(N_n + 2 - 2^i, N_n + 1)$ and $(N_n + 1, N_n + 2 - 2^i)$,

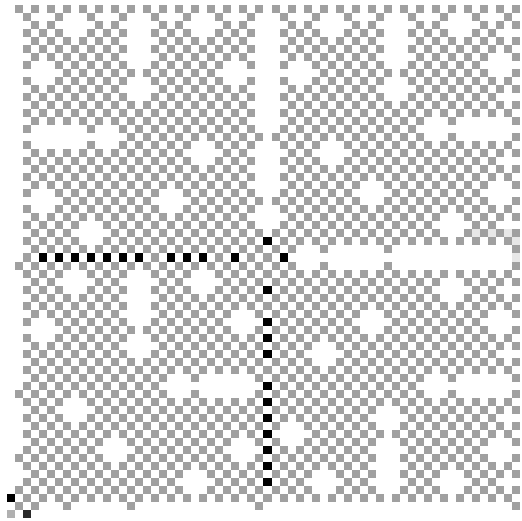

FIGURE 14
Cells added by the 4 condition of τ_{134} are darker. These boundary cells are added on every dyadic scale, then reproduced by the cloning process.

where $0 \leq i < n$, are already filled in by τ_{13}, due to the embedding of the Sierpinski lattice. This leaves $(2^n - 1) - (2n - 1)$ previously empty cells with four occupied neighbors that fill by the 4 condition, as claimed. □

Therefore

$$q_{n+1} = 4q_n + 2^n - 2n - 6,$$

which has solution

$$q_n = \frac{29}{72}4^n - 2^{n-1} + \frac{2}{3}n + \frac{20}{9}.$$

The crystal size is $a_n = 4q_n - 7$ because the 4 added cells on the axes are double counted and the origin is counted 3 times too many. It follows that

$$a_n = \frac{29}{18}4^n - 2^{n+1} + \frac{8}{3}n + \frac{17}{9},$$

and the asymptotic density of the rotated rule τ^*_{134} and original rule τ_{134} are $\rho^*_{134} = \frac{29}{72}$ and $\rho_{134} = \frac{29}{36}$, respectively.

In closing, we note that $\rho_{134} = \frac{29}{36}$ is *lower* than $\rho_{14} = 1$ even though cells join the crystal with the former density in an additional case. The lack of monotonicity in nontrivial Packard Snowflakes that produces their exotic structure also accounts for surprises such as this.

8 ACKNOWLEDGMENTS

This research was conducted by a Collaborative Undergraduate Research Lab (CURL), under the supervision of Professor David Griffeath, at the University of Wisconsin – Madison during the 2006–7 academic year. The CURL was sponsored by a National Science Foundation VIGRE award to the UW-Madison Mathematic Department. The named authors took the lead preparing this paper for publication.

REFERENCES

[1] Packard N. Lattice models for solidification and aggregation. *Institute for Advanced Study Preprint*. Reprinted (1986). *Theory and Application of Cellular Automata*, Wolfram S. (ed.). World Scientific, 305–310, 1984.

[2] Wolfram S. *A New Kind of Science*. Champaign: Wolfram Media. 2002.

[3] von Koch H. Sur une courbe continue sans tangente, obtenue par une construction géométrique élémentaire. *Arkiv för Mathematik, Astronomi och Fysik* **1** (1904), 681–702.

[4] Packard N. and Wolfram S. Two dimensional cellular automata. *Journal of Statistical Physics* **38** (1985), 901–946.

[5] Gravner J. and Griffeath D. *Modeling Snow Crystal Growth II*. To appear, 2007.

[6] Wolfram S. Computer software in science and mathematics. *Scientific American* **251** (1984), 188–203.

[7] Levy S. *Artificial Life: The Quest for a New Creation*. New York City: Pantheon Books, 1992.

[8] Gravner J. and Griffeath D. *Modeling Snow Crystal Growth III*. In preparation, 2007.

[9] Gravner J. and Griffeath D. Cellular automaton growth on Z^2: theorems, examples and problems. *Advances in Applied Mathematics* **21** (1998), 241–304.

[10] Gravner J. and Griffeath D. Modeling snow crystal growth I. *Experimental Mathematics* **15** (2006), 421–444.

[11] Wojtowicz M. *Mirek's Cellebration: a 1D and 2D Cellular Automata explorer* http://www.mirwoj.opus.chelm.pl/ca/.

[12] Sierpinski W. Sur une courbe dont tout point est un point de ramification. *C. R. A. S.* **160** (1915), 302–305.